

Reduction Method of Torque Ripple, DC Current Ripple, and Radial Force Ripple with Control Flexibility of Five-Phase SRM

Takahiro Kumagai

Dept. of Science of Technology Innovation
Nagaoka University of Technology
Nagaoka, Japan
kumagai_t1125@stn.nagaokaut.ac.jp

Jun-ichi Itoh

Dept. of Science of Technology Innovation
Nagaoka University of Technology
Nagaoka, Japan
itoth@vos.nagaokaut.ac.jp

Keisuke Kusaka

Dept. of Electrical, Electronics, and
Information Engineering
Nagaoka University of Technology
Nagaoka, Japan
kusaka@vos.nagaokaut.ac.jp

Abstract—This paper proposes a torque ripple, DC current ripple, and radial force ripple reduction method with five-phase switched reluctance motor (SRM). The proposed method makes these three ripples simultaneously zero, which is so-called “triple zero” in this paper, by improving control flexibility with five-phase. In particular, the triple zero is achieved with the same efficiency as the general driving method of SRM by utilizing the control flexibility effectively. A three-phase 18S/12P type SRM and a five-phase 20S/16P type SRM are used in finite-element analysis and experiment in order to validate the proposed method. As a result, the main components of the torque ripple, the DC current ripple, and the vibration are reduced by 92.8%, 95.5%, and –18.0dB respectively. In addition, in comparison with the single pulse-wide current drive, the current RMS in three-phase SRM is increased by 27.8% as a sacrifice of the triple zero, while the current RMS in five-phase SRM is increased by only 2.4%.

Keywords—switched reluctance motor, instantaneous current control, torque ripple, acoustic noise, vibration, DC current ripple, five-phase

I. INTRODUCTION

Recently, high-efficiency motors and high-power-density motors have been studied actively due to the expansion of electric vehicles (EVs) and hybrid electric vehicles (HEVs) [1-3]. In particular, switched reluctance motor (SRM) has attracted much attention as alternative motor for permanent magnet synchronous motor (PMSM) and induction motor (IM) thanks to its rare-earth-element free and low manufacturing cost [4][5]. However, large torque ripple, DC current ripple, and radial force ripple are major problems in the practical use of SRM. These ripples lead to acoustic noise, vibration, and deterioration of the battery lifespan. In addition, SRM has a problem of low efficiency compared with PMSM. In order to solve these problems, current control strategies have been studied actively with the development of the power electronics technology in recent year [6-17].

Single pulse-wide current drive, which controls the current to a simple rectangular, is used as a general driving method [6]. In order to improve the efficiency, the excitation timing of single pulse-wide current drive is optimized in consideration of inductance and torque characteristics [7][8]. Meanwhile, in order to reduce the torque ripple, the two-phase

excitation is applied during the switching phase interval [9][10]. On the other hand, in order to reduce the DC current ripple, the specific current waveform is introduced in order to make the magnetic energy oscillation between load and power supply theoretically constant [11][12]. In order to reduce the radial force ripple, the optimized harmonic is superimposed to the command current in order to eliminate the radial force sum of the neighboring stator poles [13][14]. In addition, the current control strategies for simultaneously reducing multiple ripples have been studied [15-18]. However, in three-phase SRM, the control flexibility during positive torque region is not enough to reduce multiple ripples simultaneously. In order to reduce multiple ripples simultaneously, it is necessary to positively use the negative torque region, which significantly increases the copper loss. As a result, the efficiency is extremely deteriorated with respect to the single pulse-wide current drive [15][16]. In order to solve this problem, there is a method of optimizing the rotor configuration for simultaneously reducing the torque ripple and the DC current ripple; however, the radial force ripple is not considered [17]. Meanwhile, there is a multi-objective optimization method in order to reduce each ripple according to its weight; however, it is impossible to reduce multiple ripples simultaneously [18].

This paper proposes a torque ripple, DC current ripple, and radial force ripple reduction method with five-phase SRM. The proposed method makes these three ripples simultaneously zero, which is so-called “triple zero” in this paper, by improving control flexibility with five-phase. The new contribution of the proposed method, the triple zero is achieved with the same efficiency as the general driving method of SRM by utilizing the control flexibility effectively.

This paper is organized as follows; first the configuration of the five-phase SRM and its control flexibilities are explained. Next, the derivation method of the ideal current waveform to achieve the zero torque ripple, zero DC current ripple, and zero radial force ripple simultaneously is explained. Finally, the finite-element analysis and experimental results are shown to validate the proposed method.

II. TRIPLE ZERO WITH FIVE-PHASE SRM

A. Structure and Specification

Fig.1 depicts the motor diagrams, whereas Table.1 shows the motor parameters of the three-phase SRM and the five-

phase SRM. For comparative verification, the five-phase SRM is designed to have the same specification and same size as our three-phase 18S/12P SRM. Note that the pole combination of the five-phase SRM is 20S/16P, which is the closest to that of the three-phase SRM. In addition, the number of turns of the five-phase SRM is adjusted to equalize the winding space factors of the three-phase SRM and the five-phase SRM.

B. Control flexibilities of SRMs

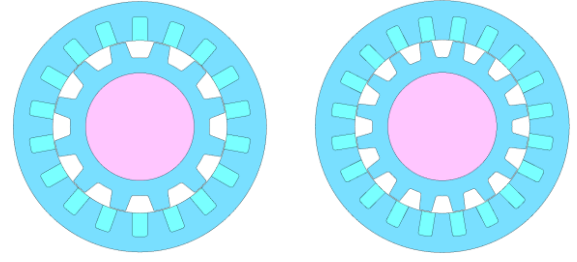
Fig.2 shows the inductance distribution and torque characteristic, and the conduction regions which are necessary to achieve the zero torque ripple, zero DC current ripple, and zero radial force ripple simultaneously in three-phase SRM and five-phase SRM. The reluctance torque is generated by the variation of magnetic resistance, i.e. inductance, according to the change of rotor position. In the single pulse-wide current drive; first, the current is raised to the reference level in the small inductance period $[\theta_M, \theta_J]$, then, the current is controlled to the constant in the positive torque ($dL/d\theta_m > 0$) period $[\theta_I, \theta_K]$, finally, the current is decayed to the zero before the negative torque ($dL/d\theta_m < 0$) start angle θ_N . This is because a large torque is obtained efficiently by raising the current with the limited input voltage of the inverter. On the other hand, in order to achieve the triple zero, three control flexibility is required, i.e. it is necessary to always energize three phases simultaneously. In three-phase SRM, it means continuous energization during one cycle; thus, the use of the negative torque ($dL/d\theta_m < 0$) period $[\theta_N, \theta_M]$ is required. As a result, the driving method for triple zero in three-phase SRM is far off from the single pulse-wide current drive, and the current RMS is extremely increased, which is not practical use. Meanwhile, in five-phase SRM, the energization of three phases is achieved by energizing only the 3/5 period of one cycle; thus, the use of the negative torque period is not required. As a result, the triple zero is achieved with the same efficiency as the single pulse-wide current drive in five-phase SRM.

C. Derivation of Ideal current waveform for Triple Zero

The ideal current waveform to achieve the zero torque ripple, zero DC current ripple, and zero radial force ripple simultaneously is derived based on the optimization method of the current waveform which consists of dc and some harmonic components [13-16]. In this method, first, torque and radial force expression are approximated with Fourier series with parameters as a function of motor current in consideration of magnetic saturation, next, the motor current is derived to minimize the variation of the torque or radial force sum with the proper approximation by numerical analysis. In order to reduce the DC current ripple as well as torque ripple and radial force ripple, DC current has to be expressed as a function of the motor current. If the winding resistance is ignored, DC current i_{DC} is expressed as in (1).

$$\begin{aligned} i_{DCx}(\theta_m) &= \frac{1}{E_{dc}} \left(i_x(\theta_m) \frac{d\Phi(i_x, \theta_m)}{dt} \right) \\ &= \frac{\omega}{E_{dc}} \left(i_x(\theta_m) \frac{\partial \Phi(i_x, \theta_m)}{\partial \theta_m} + i_x(\theta_m) \frac{di_x(\theta_m)}{d\theta_m} \frac{\partial \Phi(i_x, \theta_m)}{\partial i_x} \right) \end{aligned} \quad (1)$$

Where ω is the rotation speed, E_{dc} is the input voltage, i_x is the motor current, Φ is the flux linkage, and the subscript x indicates the phase in SRM. The flux linkage Φ can be approximated with Fourier series with parameters as a



(a) Three-phase 18S/12P SRM (b) Five-phase 20S/16P SRM

Fig. 1. Examples of general forms of SRMs.

TABLE I. MOTOR PARAMETERS OF SRMS.

	Three-phase 18S/12P SRM	Five-phase 20S/16P SRM
Rated power P_m	5.5 kW	
Rated speed ω_h	12000 r/min	
Rated torque T_n	9.3 Nm	
Input voltage	48V	
Number of poles	Stator 18, Rotor 12	Stator 20, Rotor 16
Number of turns	12 turns	11 turns
Winding resistance	0.012Ω	0.018Ω

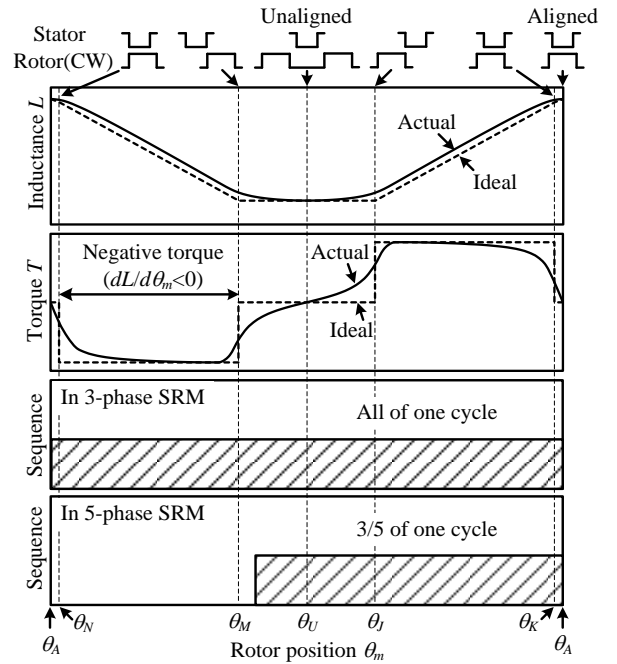


Fig. 2. The inductance distribution and torque characteristic, and the conduction regions which are necessary to achieve the zero torque ripple, zero DC current ripple, and zero radial force ripple in three-phase SRM and five-phase SRM.

function of current in consideration of magnetic saturation. In addition, the differential term of (1) can be formulated by differentiating $i(\theta_m)$ or $\Phi(i, \theta_m)$ given as mathematical expressions. The DC current ripple i_{DCrip} is obtained by subtracting $T^* \omega$ which is the average input power from the sum of the DC current i_{DCx} of all phase, and is expressed as in (2).

$$i_{DCrip}(\theta_m) = \sum_{x=A}^{CorE} i_{DCx}(\theta_m) - \frac{T^* \omega}{E_{dc}} \quad (2)$$

Where the range of the summation in three-phase SRM is from A-phase to C-phase, while that in five-phase SRM is from A-phase to E-phase. The DC current ripple RMS can be derived by computing the root mean square of (2). In order to reduce the DC current ripple as well as torque ripple and radial force ripple, the current is derived to minimize the (2) by numerical analysis.

In this paper, the ideal current waveform to achieve the triple zero is derived by optimizing the current amplitude and phase of each order of the harmonic current. In the three-phase SRM, the ideal current waveform is expressed as in (3) [13-16].

$$i(\theta_e) = i_0 + \sum_{n=1}^N i_n \sin(n\theta_e + \varphi_n) \quad (3)$$

Where θ_e is electric position, i_n and φ_n are the amplitude and phase of n-order harmonic current, and N is the highest order of the current harmonic. On the other hand, in the five-phase SRM, the current value have to be zero at both the turn-on angle θ_o and the end of conduction angle θ_c . In this paper, θ_c is set to the aligned angle θ_A with reference to the single pulse-wide current drive [6-8]. On the other hand, θ_o is set to $\theta_A - 3/5 * 2\pi/N_r$ in order to achieve the energization of three phases. Therefore, in the five-phase SRM, the ideal current waveform is expressed as in (4).

$$i(\theta_e) = \begin{cases} \sum_{n=1}^N i_n \sin \left\{ n \frac{N_r}{2} \frac{5}{3} \left(\theta_e - \frac{2}{5} \frac{2\pi}{N_r} \right) \right\} & \frac{2}{5} \frac{2\pi}{N_r} \leq \theta_e \leq \frac{2\pi}{N_r} \\ 0 & \text{otherwise} \end{cases} \quad (4)$$

III. FINITE-ELEMENT ANALYSIS AND EXPERIMENT RESULT

In this section, first, the ideal current waveform is derived based on the method explained in Section II, next, the derived current is applied in FEM analysis and experiment. Note that the ideal current waveform is optimized with Generalized Reduced Gradient (GRG) method to make each ripple rate 5% or less and minimize the motor current RMS. The reason for choosing 5% is that a few percent of the ripple occurs due to the approximation error [13-16].

Fig.3 shows the ideal current waveform to achieve the triple zero in three-phase SRM and five-phase SRM. In the three-phase SRM, negative torque is generated, and is compensated by larger torque than the torque reference from the other phase, resulting to large current. Meanwhile, in the five-phase SRM, no negative torque is generated, and the torque makes constant by sharing by each phase without the wasted current.

A. Finite-Element Analysis

Fig.4 shows the FEM analysis results of the current waveforms, the torque, the DC current, the radial force, and the current RMS with the single pulse-wide current drive (SPCD) and the ideal current waveform drive (ICWD) in the three-phase SRM and the five-phase SRM. In both of the three-phase SRM and the five-phase SRM, these ripples are reduced by around 90% with ICWD compared with SPCD. In addition, the current RMS in three-phase SRM is increased by 24.2% as a sacrifice of the triple zero, while the current RMS in five-phase SRM is increased by only 1.7%. Therefore, in FEM analysis, it is confirmed that the triple zero is achieved

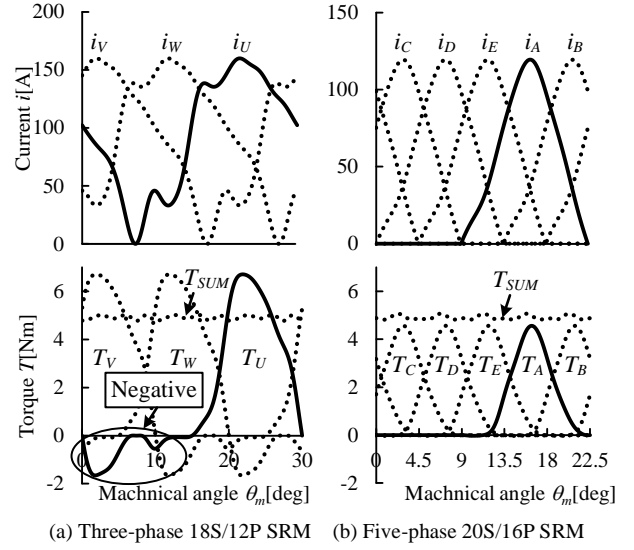
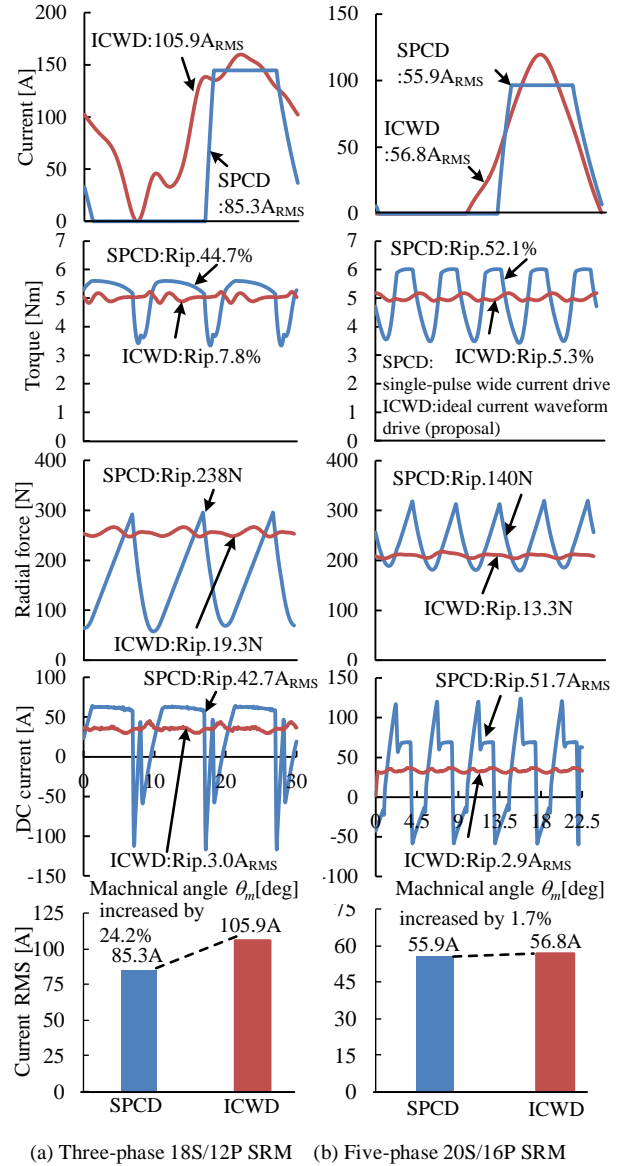
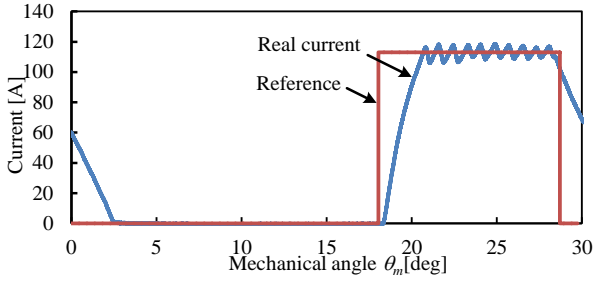


Fig. 3. Ideal current waveforms and calculated torque.

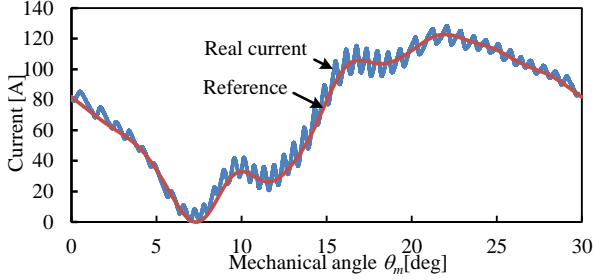


(a) Three-phase 18S/12P SRM (b) Five-phase 20S/16P SRM

Fig. 4. FEM results of waveforms of the current, the torque, DC current, radial force, current RMS in cases of single pulse-wide current and ideal current at $T^*=4.91\text{Nm}$, $\omega=2400\text{r/min}$.



(a) Single pulse-wide current drive (SPCD)



(b) Ideal current waveform drive (ICWD)

Fig. 5. Measured currents of the three-phase SRM in cases of single pulse-wide current and ideal current at $T^*=3\text{Nm}$, $\omega=2866\text{r/min}$ in the experiment.

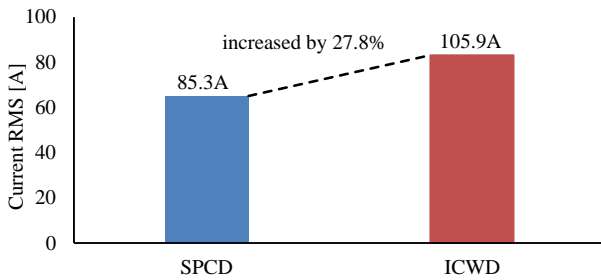


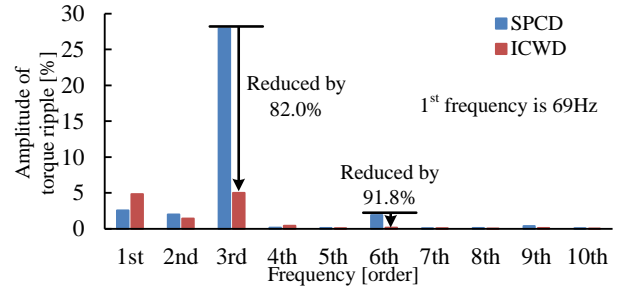
Fig. 6. Comparison of motor current RMS of the three-phase SRM in cases of single pulse-wide current and ideal current.

with the same efficiency as the general driving method by utilizing the control flexibility.

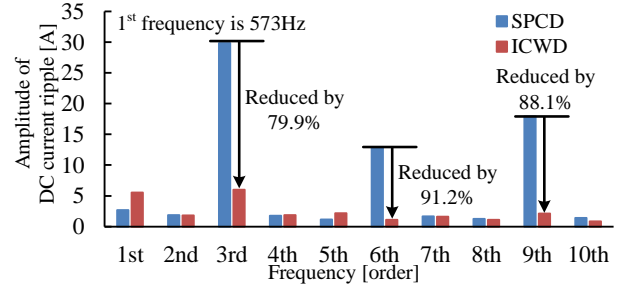
B. Experiment Result

The effectiveness of the proposed method is confirmed by experiment with the three-phase SRM and the five-phase SRM. In order to realize high-speed current control and reduce the ripples caused by the hysteresis error, current-hysteresis controller is constructed by analog circuit. Due to the limitation of cutoff frequency of the torque meter and avoidance of torsional resonance of test bench, the torque ripple is measured at low speed. Note that fundamental motor current frequency f_i is $N_p N / 60$. In addition, the main components of the ripples of three-phase SRMs are $3f_i$, $6f_i$, $9f_i$, and so on. Meanwhile, those of five-phase SRMs are $5f_i$, $10f_i$, $15f_i$, and so on. Therefore, the ripple frequency of the five-SRM is higher than that of the three-phase SRM. This results in the experiment at lower speed with five-phase SRM.

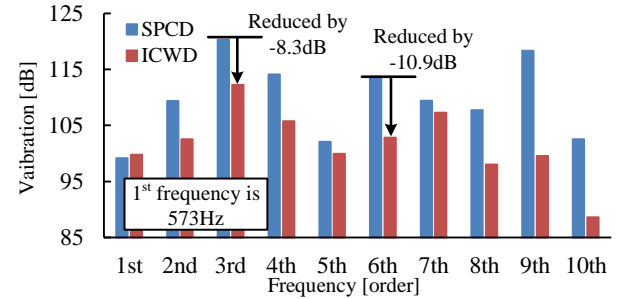
Fig.5 shows the measured currents of the three-phase SRM with the single pulse-wide current drive (SPWD) and ideal current waveform drive (ICWD) in the experiment. In SPWD, the motor current is a trapezoidal as shown in Fig.7 (a). On the other hand, in ICWD, the motor current follows the ideal current reference accurately as shown in Fig.5 (b).



(a) Torque ripple



(b) DC current ripple



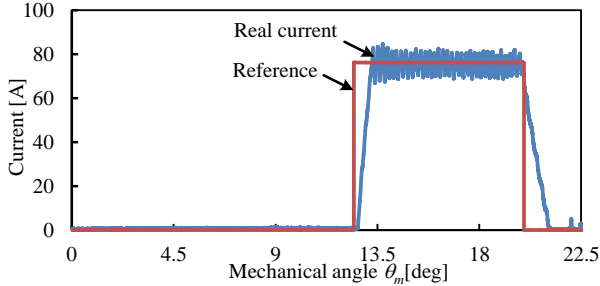
(c) Vibration acceleration

Fig. 7. Experimental results of the torque ripple, DC current ripple, and vibration of three-phase SRM in cases of single pulse-wide current and ideal current at $T^*=3\text{Nm}$. Note that ω is 345r/min in the torque ripple measurement, while ω is 2866r/min in the others due to the limitation of cutoff frequency of the torque meter and avoidance of torsional resonance of test bench

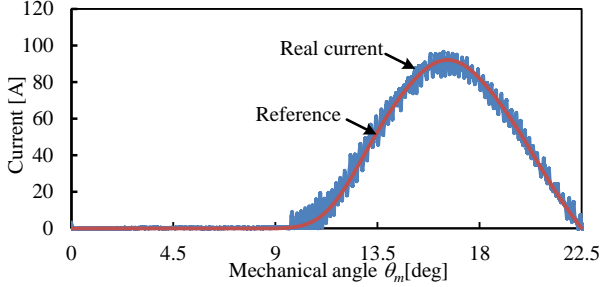
Fig.6 shows the comparison results of motor current RMS of the three-phase SRM in cases of single pulse-wide current and ideal current. The current RMS of ICWD is increased by 27.8% compared with SPWD as a sacrifice of the triple zero. In other word, the copper loss is increased by 63.3%, which is not practical use.

Fig.7 shows the experimental results of the harmonic components of the torque ripple, the DC current ripple, and the vibration acceleration with SPCD and ICWD in the three-phase SRM. The main components of the torque ripple, the DC current ripple, and the vibration are reduced by 82.0%, 79.9%, and -8.3bB respectively by ideal current waveform. Therefore, in experiment, the effectiveness of the ideal current waveform is confirmed in three-phase SRM.

Fig.8 shows the measured currents of the three-phase SRM with the single pulse-wide current (SPWD) and ideal current waveform drive (ICWD) in the experiment. In SPWD, the motor current is a trapezoidal as shown in Fig.7 (a). On the other hand, in ICWD, the motor current follows the ideal current reference accurately as shown in Fig.5 (b).



(a) Single pulse-wide current drive (SPCD)



(b) Ideal current waveform drive (ICWD)

Fig. 8. Measured currents of the three-phase SRM in cases of single pulse-wide current and ideal current at $T^*=3\text{Nm}$, $\omega=1200\text{r/min}$ in the experiment.

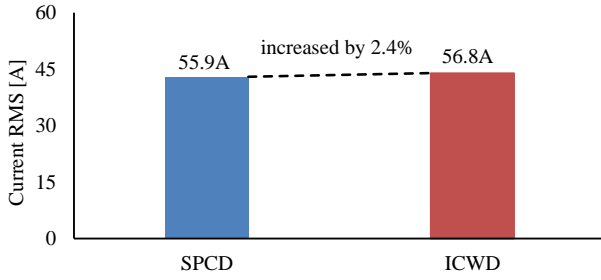
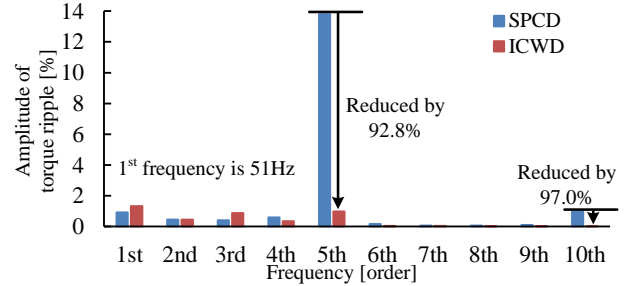


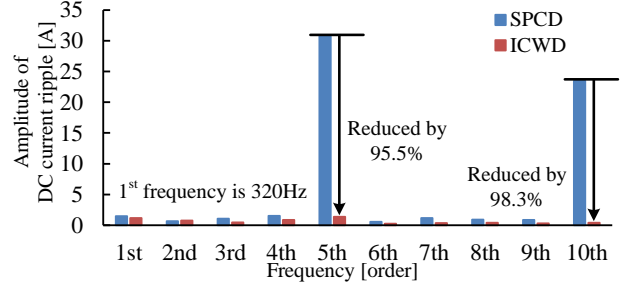
Fig. 9. Comparison of motor current RMS value of the three-phase SRM in cases of single pulse-wide current and ideal current.

Fig.9 shows the comparison results of motor current RMS of the five-phase SRM in cases of single pulse-wide current and ideal current. The current RMS of ICWD is increased by only 2.4% compared with SPWD. In other word, the copper loss is increased by only 4.9%, which is low sacrifice as the triple zero and practical use.

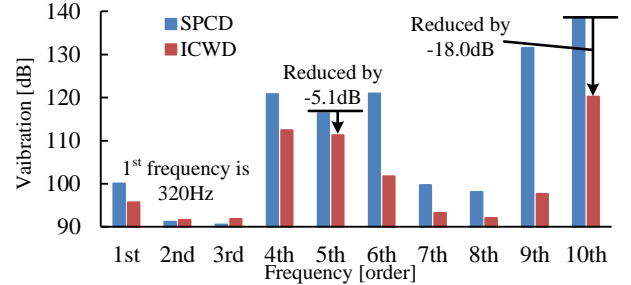
Fig.10 shows the experimental results of the harmonic components of the torque ripple, the DC current ripple, and the vibration acceleration with the single pulse-wide current drive and the ideal current waveform in the five-phase SRM. The main components of the torque ripple, the DC current ripple, and the vibration are reduced by 92.8%, 95.5%, and -18.0dB respectively by ideal current waveform. Therefore, in experiment, the effectiveness of the ideal current waveform is confirmed in five-phase SRM. In addition, these ripple reduction are achieved with the almost same copper loss as SPCD as shown in Fig.9. Therefore, torque ripple, DC current ripple, and vibration caused by radial force ripple, which are major problems in the practical use of SRM, are reduced with the same efficiency as the general driving method of SRM by utilizing the improved control flexibility with five-phase SRM effectively.



(a) Torque ripple



(b) DC current ripple



(c) Vibration acceleration

Fig. 10. Experimental results of the torque ripple, DC current ripple, and vibration of three-phase SRM in cases of single pulse-wide current and ideal current at $T^*=3\text{Nm}$. Note that ω is 191r/min in the torque ripple measurement, while ω is 1200r/min in the others due to the limitation of cutoff frequency of the torque meter and avoidance of torsional resonance of test bench.

IV. CONCLUSION

In this paper, the reduction method of a torque ripple, DC current ripple, and radial force ripple with five-phase switched reluctance motor has been proposed. The proposed method makes these three ripples simultaneously zero, which is so-called “triple zero” in this paper, by improving control flexibility with five-phase. In particular, the triple zero is achieved with the same efficiency as the general driving method of SRM by utilizing the control flexibility effectively. A three-phase 18S/12P type SRM and a five-phase 20S/16P type SRM are used in finite-element analysis and experiment in order to validate the proposed method. The main components of the torque ripple, the DC current ripple, and the vibration are reduced by 92.8%, 95.5%, and -18.0dB respectively by proposed current drive method. In addition, in comparison with the single pulse-wide current drive, the current RMS in three-phase SRM is increased by 27.8% as a sacrifice of the triple zero, while the current RMS in five-phase SRM is increased by only 2.4%.

REFERENCES

- [1] Y. Enomoto, K. Deguchi, T. Imagawa, "Development of an Ultimate-high-efficiency Motor by utilizing High-Bs Nanocrystalline Alloy", *IEEJ Journal of Industry Applications*, vol. 9, no. 1, pp. 102-108 (2020)
- [2] N. G. M. Thao, N. Denis, Y. Wu, S. Odawara, and K. Fujisaki, "Study of the Effect of Load Torque on the Iron Losses of Permanent Magnet Motors by using Finite Element Analysis", *IEEJ Journal of Industry Applications*, vol. 8, no. 3, pp. 522-531 (2019)
- [3] K. Yamazaki and H. Narushima, "Procedure for Optimization of Interior Permanent Magnet Synchronous Motors with Concentrated Windings by Considering End-Leakage Flux", *IEEJ Journal of Industry Applications*, vol. 8, no. 5, pp. 820-826 (2019)
- [4] A. Chiba, H. Hayashi, K. Nakamura, S. Ito, K. Tungpimolrut, T. Fukao, M. A. Rahman, and M. Yoshida, "Test Results of an SRM Made From a Layered Block of Heat-Treated Amorphous Alloys", *IEEE Transactions on Industry Applications*, Vol.44, No.3, pp.699-706 (2008)
- [5] H. Hayashi, K. Nakamura, A. Chiba, T. Fukao, K. Tungpimolrut, and D. G. Dorrell, "Efficiency Improvements of Switched Reluctance Motors With High-Quality Iron Steel and Enhanced Conductor Slot Fill", *IEEE Transactions on Energy Conversion*, Vol.24, No.4, pp.819-825 (2009)
- [6] Miller T. J. E.: *Electronic Control of Switched Reluctance Machines*, pp.74-97, Newnes (2001)
- [7] C. Mademlis and I. Kioskeridis, "Performance optimization in switched reluctance motor drives with online commutation angle control", *IEEE Transactions on Energy Conversion*, Vol. 18, No. 3, pp. 448-457 (2003)
- [8] I. Kioskeridis and C. Mademlis, "Maximum efficiency in single-pulse controlled switched reluctance motor drives", Vol. 20, No. 4, pp. 809-817 (2005)
- [9] J. Ye, B. Bilgin, and A. Emadi, "An Offline Torque Sharing Function for Torque Ripple Reduction in Switched Reluctance Motor Drives", *IEEE Transactions on Energy Conversion*, Vol. 30, No. 2, pp. 726-735 (2015)
- [10] H. Li, B. Bilgin, and A. Emadi, "An Improved Torque Sharing Function for Torque Ripple Reduction in Switched Reluctance Machines", *IEEE Transactions on Power Electronics*, Vol. 34, No. 2, pp. 1635-1644 (2019)
- [11] L. Du, B. Gu, J. S. Lai, and E. Swint, "Control of pseudo-sinusoidal switched reluctance motor with zero torque ripple and reduced input current ripple," in *IEEE ECCE2013*, pp. 3770-3775 (2013)
- [12] T. Kusumi, K. Kobayashi, K. Umetani, and E. Hiraki, "Analytical Derivation of Phase Current Waveform Eliminating Torque Ripple and Input Current Ripple of Switched Reluctance Motors under Magnetically Saturated Operation" in *IEEE ECCE2019*, pp.6540-6547 (2019)
- [13] M. Takiguchi, H. Sugimoto, N. Kurihara, and A. Chiba, "Acoustic noise and vibration reduction of SRM by elimination of third harmonic component in sum of radial forces", *IEEE Trans. Energy Convers*, Vol.30, No.3 pp.883-891 (2015)
- [14] J. Furqani, M. Kawa, K. Kiyota, and A. Chiba, "Current Waveform for Noise Reduction of a Switched Reluctance Motor under Magnetically Saturated Condition", *IEEE Transactions on Industry Applications*, Vol.54, No.1 pp.213-222 (2018)
- [15] M. Kawa, K. Kiyota, J. Furqani, and A. Chiba, "Acoustic Noise Reduction of a High-Efficiency Switched Reluctance Motor for Hybrid Electric Vehicles With Novel Current Waveform" *IEEE Transactions on Industry Applications*, Vol.55, No.3 pp.2519-2528 (2019)
- [16] J. Furqani, M. Kawa, C. A. Wiguna, N. Kawata, K. Kiyota, and A. Chiba, "Current Reference Selection for Acoustic Noise Reduction in Two Switched Reluctance Motors by Flattening Radial Force Sum", *IEEE Transactions on Industry Applications*, Vol.55, No.4 pp.3617-3629 (2019)
- [17] T. Kusumi, T. Hara, K. Umetani, and E. Hiraki, "Rotor Configuration Which Reduces Copper Loss of Switched Reluctance Motors With Suppression of Torque Ripple and Input Current Ripple" in *IEEE ECCE2018*, pp.6097-6103 (2018)
- [18] T. Kumagai, K. Kusaka, and J. Itoh, "Reduction Method of Current RMS Value, DC Current Ripple, and Radial Force Ripple for SRM based on Mathematical Model of Magnetization Characteristic", in *IEEE IFEEC2019*, No. 1123 (2019)